J Mater Sci (2007) 42:6701–6707
DOI 10.1007/s10853-006-1493-6

Fracture behavior and microstructure of steel fiber reinforced cast iron

Mehmet Şimşir

Received: 5 November 2006 / Accepted: 28 December 2006 / Published online: 30 April 2007

Abstract In this study, improvement of fracture toughness and strength of gray cast iron by reinforcing steel fiber was investigated. Three point bend specimens were used to calculate the flexural strength and fracture toughness. Fracture toughness of the reinforced cast iron with two distinct volume fraction (Vf = 0.05 and 0.08) were calculated by compliance method and *J*-integral method using single specimen technique. The study shows that fiber reinforced composite has higher fracture toughness and flexural strength than cast iron without reinforcement. Also, fracture toughness increases with increasing volume fraction of reinforcement. Optical and scanning electron microcopy (SEM) analyses were used to examine the microstructure and fracture surface. It is noted that the carbon diffuses from gray cast iron to steel fiber and graphite free transition regions with high hardness were observed due to the carbon diffusion.

Introduction

There has been significant effort to explore the potential use of ductile phase reinforcement in the toughening of relatively brittle metal matrix. Antolovich et al. [1, 2] studied on fracture toughness of the tough maraging steel reinforced (as continuous fiber and laminated) in maraging steel but relatively brittle. Akdemir et al. [3] worked on the improvement of strength and toughness of metal matrix composites (MMCs) consisted of ductile reinforcement relatively brittle matrix composite system.

Fracture Behavior of MMC explained by several micromechanical failure mechanisms. These mechanisms include fiber breakage, matrix damage, fiber/matrix debonding, fiber pull-out etc. Antolovich et al. [1] showed the improvement of fracture toughness of MMC by fiber/matrix debonding. Soboyejo et al. [4] explained fracture toughness of fiber reinforced MMC by crack tip blunting and crack bridging mechanisms. Chiang [5] worked on the crack resistance behavior (R-curve) fiber reinforced in the polymer matrix composites and increasing fracture toughness is attributed to fiber pull out mechanism. Qin and Zhang [6] studied on toughening mechanism of the metal rod reinforced in Al alloy matrix and fracture behavior was explained by deformation of matrix and interface debonding.

One of the most important factors in the fabrication of MMCs is compatibility (wettability and reactivity) between the matrix and reinforcement. Wetting and interfacial reactions determine the quality of the bond between components, and therefore greatly influence the final properties of the composites [7].

The first aim of this study is to produce high toughness and high strength MMC consisted of high toughness and strength steel fiber reinforced in relatively low toughness and strength gray cast iron. The second benefit of this composite system is to remove graphite flakes which behave like cracks in the matrix by diffusion of carbon atoms from gray cast iron (matrix) to low carbon steel fibers (reinforcements). Hence, the microstructure and the mechanical properties of MMCs comprising castings of gray cast iron with steel wire reinforcement have been examined.

M. Şimşir (✉)
Department of Metallurgical and Materials Engineering,
Cumhuriyet University, Sivas 58140, Turkey
e-mail: msimsir@cumhuriyet.edu.tr

Experimental study

Materials

The composites consist of steel fibers (tough phase) as reinforcement and cast iron (brittle phase) as matrix. The chemical composition of steel fiber is 0.4 %C, 0.14 %Mn and 0.15 %Si and steel fiber is used as filler material in welding in commercially. The cast iron as a matrix is 3.35 %C, 1.52 %Si, 0.61 %Mn, 0.00165 %S and 0.00100 > %P in chemical composition. The composites were produced by sand mold casting technique. For the production of composites, sand mold with 25 × 50 × 230 mm in dimensions were used to produce castings. Steel wires with 4 mm in diameter were set in the mold in two different wire orientations, 2 × 3 and 3 × 3 (Fig. 1). By this way, two different volume fraction of reinforcement, $V_f = 0.05$ and $V_f = 0.08$ were produced in the composites. The casting temperature was chosen to be 1,350° C and followed by cooling in the sand mold. In order to compare the fracture behavior of the gray cast iron and the composites, the gray cast iron and the composites were casted in the same casting conditions and dimensions.

Three point bending specimens were prepared for the cast iron and composites according to ASTM E-399 standard. Test speed is 0.01 mm s^{-1} under stroke control. Figure 2 shows the stress-strain curve for composite with $V_f = 0.08$. Three point bend test was applied five times for each specimen to calculate the flexural strength (σ).

Measurement of fracture toughness

Fracture toughness of the fiber reinforced composites and the cast iron without reinforcement were measured in terms of K_{IC} and J_{IC}-Integral. In linear elastic behavior, several methods have been developed to determine the plain strain fracture toughness K_{IC}, including the compliance technique

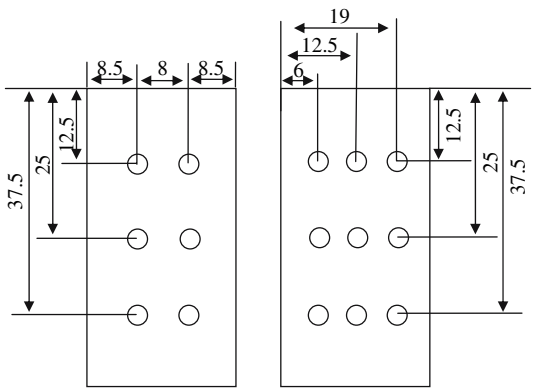

Fig. 1 Schematic illustration of stacking of fibers in the matrix (all dimensions in mm)

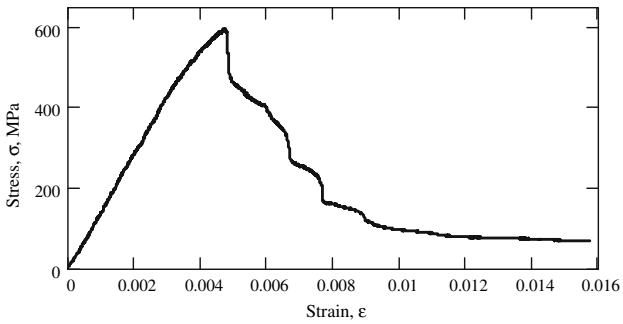

Fig. 2 Stress–strain curves of the composites with $V_f = 0.08$

[8], the initial notch depth method [9], and crack tip opening displacement method [10]. In elastic-plastic behavior, to determine fracture toughness, J_{IC}, deep crack sample technique [11], notched versus unnotched sample technique [12], resonant frequency test [13], unloading compliance method [14], and potential drop technique [15], have been developed.

Compliance method for Kıc

In this study, K_{IC} was determined single specimen compliance technique was used. Three point bend specimens were produced according to ASTM E399 standard. Three point bend specimens were machined with dimensions 220 × 44 × 22 mm for initial crack length to width ratio, $a_o/W = 0.38$ and a width to thickness ratio (W/B) of 2 as shown in Fig. 3. The crack of 16.7 mm was opened by using wire erosion machine using brass wire 0.25 mm in diameter. Since the composite is brittle, prefatigue was not applied to produce sharp crack. Samples were tested in a hydraulic test machine under stroke control 0.01mm s^{-1} of crosshead speed [16]. The test was replicated three times for each specimen.

The specimen was loaded and unloaded in a sequence such that at each step load line displacement was 0.1 mm higher than the previous loading. At unloading, the displacement was decreased minimum possible loading without changing in the load line. A relaxation time of 60 s. was used at each step of loading and unloading.

The crack length was measured by taking photograph at each loading in the range of relaxation time and also traveling microscopy from the surfaces of the specimen.

From the sequence of loading and unloading described above, data on load–load line displacement were recorded. From these data, plain strain fracture toughness, K_{IC} was determined via compliance method. The compliance, C_i, at the unloading is defined as

$$C_i = \frac{\Delta\delta}{\Delta P} \quad (1)$$

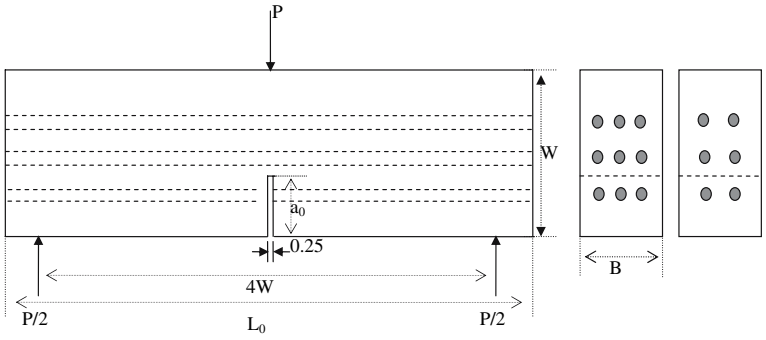

Fig. 3 Schematic illustration of three point bend specimen for $a_o/W = 0.38, W/B = 2$ (all dimensions are in mm)

where $\Delta\,\delta$ is the change in load line displacement and ΔP is the change in load during unloading. After C_i, graph of compliance- a/W were obtained and compliance equation for a/W ratio was found.

Plain strain fracture toughness were determined from the following equation

$$K_{IC} = \left[\frac{E_{eff}}{(1-v^2)}\frac{P_{\max}^2}{2BW}\frac{dC}{d\left(\frac{a}{W}\right)}\right]^{\frac{1}{2}} \tag{2}$$

where $P_{\max}$ is the max load which was determined load–load line deflection curves at the each loading, v is the Poisson ratio, B is the thickness, W is the width of the specimen and E_{eff} is the effective Elastic Modulus,

$$E_{eff} = \frac{1}{E} \tag{3}$$

$$E = \left(\frac{a_{22}a_{11}}{2}\right)^{\frac{1}{2}}\left[\left(\frac{a_{22}}{a_{11}}\right)^{\frac{1}{2}} + \left(\frac{a_{66}+2a_{11}}{2a_{11}}\right)\right]^{\frac{1}{2}} \tag{4}$$

$$a_{11} = \frac{1}{E_1} \quad a_{22} = \frac{1}{E_2} \quad a_{21} = a_{12} = \frac{-v_{12}}{E_1} = \frac{-v_{21}}{E_2} \quad a_{66} = \frac{1}{G_{12}} \tag{5}$$

$$E_1 = V_f E_f + \left(1 - V_f\right)E_m \tag{6}$$

$$E_2 = \frac{E_f E_m}{V_f E_m + \left(1 - V_f\right)E_f} \tag{7}$$

$$G_{12} = \frac{G_f G_m}{V_f G_m + \left(1 - V_f\right)G_f} \tag{8}$$

$$v_{12} = V_f v_f + \left(1 - V_f\right)v_m \tag{9}$$

where, E_1 and E_2 are the Elastic Modulus of composite in fiber direction and transverse direction respectively. E_{m} and E_{f} are the Elastic Modulus of matrix and fiber respectively. G_{12}, G_{f} and G_{m} are the shear modulus of composite, fiber and matrix respectively. v_{12}, v_{f} and v_{m} are the Poisson's ratio of composite, fiber and matrix, respectively.

J-integral method for Jıc

J-Integral method can be applied to determine fracture toughness of fiber reinforced composite materials. This method is based on determination of an energy, which expresses the change in potential energy when a crack extends one unit. That is,

$$J = -\frac{1}{B}\frac{dU}{da} \tag{10}$$

where, U is the potential energy, a is the crack length of the material.

In this study, notched and unnotched samples technique was preferred to obtain the fracture toughness. Fracture toughness, J_{IC}, was calculated by subtracting the strain energy area under the load–load line displacement curve of the notched specimen from the area under the load–load line displacement curve of the same type of unnotched specimen.

$$J_{ıc} = \frac{2(A_n - A_u)}{B(W-a)} \tag{11}$$

where, A_{n} and A_{u} are the strain energies of the notched and unnotched specimens, respectively.

To estimate fracture toughness of a nonlinear elastic body, J_{IC} has been proposed when linear elastic behavior predominates, J integral directly related to the K_{IC} through the following equation,

$$K_{IC}^2 = \left(\frac{E_{eff}}{1-v^2}\right)J_{IC} \tag{12}$$

Results and discussion

To investigate the mechanical properties of gray cast iron and composite materials with two distinct volume fractions(with $V_{\text{f}} = 0.05$ and $V_{\text{f}} = 0.08$), three point bend

specimens were prepared for with and without reinforced cast iron. The effect of volume fraction of the fiber was examined on the flexural strength of gray cast iron and composite materials. The results are shown on Fig. 4 and each point on the the figure is the average of the five specimens. The current results show that there is an increase in flexural strength with increasing volume fraction of the fiber. Similar results were obtained by Akdemir et al. [3]. The gray cast iron without fiber reinforced has a flexural strength of $421\,\mathrm{Nmm}^{-2}$. Flextural strength of composites with $V_f = 0.05$ and $V_f = 0.08$ were 40.6% and 55.1% greater than that of gray cast iron without fiber respectively.

Fracture toughness

Load–load line displacement curve was obtained for composite with $V_f = 0.08$ (Fig. 5) and similar curves for $V_f = 0.05$ and cast iron (matrix) without reinforcement. As shown in Fig. 5, the load increases linearly up to third reloading due to elastic deformation and slope of curve decreases until reaching maximum load because fibers carry the load and deform plastically. After that since first row of fiber breaks, load decreases suddenly.

Figure 6 shows the graph of compliance (C) versus crack length to width ratio (a/W) for composite with $V_f = 0.08$. Compliance was calculated from the unloading path of load–load line displacement graph. A third degree polynomial function was obtained from C-(a/W) graph. Compliance equation for the composite with $V_f = 0.08$ for the a/W ratio between 0.38 and 0.81 was founf as follows,

$$C = 2 \times 10^{-6}\left(\frac{a}{W}\right)^3 - 2 \times 10^{-6}\left(\frac{a}{W}\right)^2 + 9 \times 10^{-7}\left(\frac{a}{W}\right) - 1 \times 10^{-7} \quad (13)$$

Validity of compliance method depends on the correct measurement of compliance of the specimen. It is expected that residual stresses setup in matrix or reinforcement or interface, relaxation in the composites should be more complex than that in the monolithic material. Sufficient relaxation time was allowed otherwise compliance may be calculated underestimated or overestimated [14, 17]. For this purpose, the crosshead was stopped for 60 s before unloading/loading and load relaxation was observed.

K_{IC} values were calculated from compliance method, Table 1. Fracture toughness of the cast iron without reinforcement was calculated $18.30\,\mathrm{MNm}^{-1.5}$ and that of the composite with $V_f = 0.08$ was $78.85\,\mathrm{MNm}^{-1.5}$. It is noted that fracture toughness of the gray cast iron increases with reinforcing steel wires [3]. K_{IC} of the composite with $V_f = 0.08$ and $V_f = 0.05$ is 336.4% and 88.1% greater than that of gray cast iron without reinforcement, respectively. It

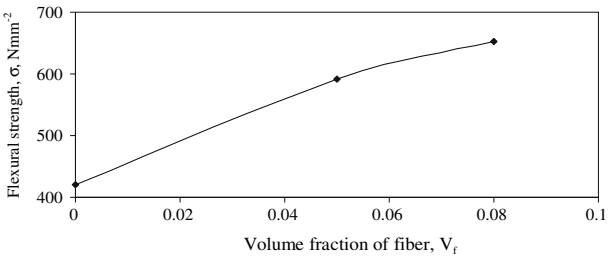

Fig. 4 The effect of volume fraction of the fiber on the flexural strength

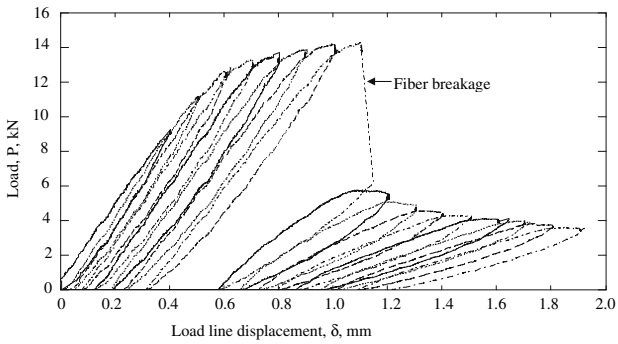

Fig. 5 Load–load line displacement curve of composite with $V_f = 0.08$ for compliance method

Fig. 6 Variation of compliance with crack length to width ratio (a/W) for $V_f = 0.08$

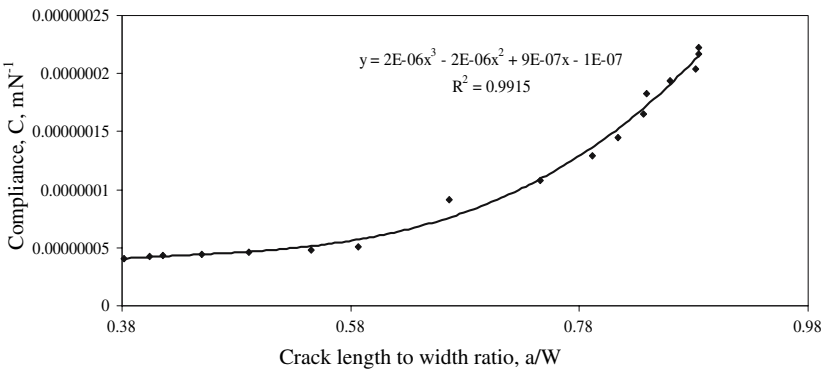

Table 1 Fracture toughnesses of the materials obtained from compliance and *J*-integral methods

Material	Compliance method, K_{IC}, $MNm^{-1.5}$	*J*-integral method	
		J_{IC}, kNm^{-1}	K_{IC} (from Eq. 8), $MNm^{-1.5}$
Cast iron (matrix)	18.30		
Composite with $V_f = 0.05$	34.42	9.57	36.11
Composite with $V_f = 0.08$	78.85	42.1	75.13

is seen that fracture toughness, K_{IC}, increases with increasing volume fraction of the reinforcement. The reinforcing fiber is high tough and strength and the matrix is brittle material. Similar results were obtained by Gerberich [18], Antolovich et al. [1] and Soboyejo et al. [4] for similar composite systems.

Critical *J* integral value, (J_{IC}), was calculated by subtracting the strain energy area under the load–load line displacement curve of the notched specimen from the area under the load–load line displacement curve of the same type of unnotched specimen. Total area under the load–load line displacement curve was determined by using trapezoidal rule. Figure 7 shows the load–load line displacement for notched and unnotched composite with $V_f = 0.08$.

As shown in Table 1, fiber reinforced composite with $V_f = 0.05$ has a fracture toughness value of $J_{IC} = 9.57\,kNm^{-1}$ and that with $V_f = 0.08$ has a value of $J_{IC} = 42.10\,kNm^{-1}$. Fracture toughness of the fiber reinforced composite, J_{IC}, increases with increasing volume fraction of the reinforcement. Fracture toughness of composites with $V_f = 0.08, J_{IC}$ were 336.9% greater than that of the composite with $V_f = 0.05$.

K_{IC} values were calculated from the Eq. (12). Plain strain fracture toughness K_{IC} calculated from either compliance or *J*-integral method. These results show that these two values does not change significantly. K_{IC} values of composite with $V_f = 0.05$ is 36.11 and $34.42\,MNm^{-1.5}$ calculated from *J*-integral and compliance method, respectively. K_{IC} values of composite with $V_f = 0.08$ is 75.13 and $78.85\,MNm^{-1.5}$ calculated from *J*-integral and compliance method, respectively.

Fracture surfaces of the test specimens were examined by Scanning electron microscopy (SEM). Carbon takes place as graphite flakes in the gray cast iron (Fig. 10b) and graphite is a brittle material. Tip of graphite flakes behave as notch in the cast iron. When load is applied, stress concentration increases at the tips of the flakes and the cracks form at the tips of the flakes and start to propagate into the cast iron. Therefore, fracture toughness of cast iron is not so high due to graphite in flake shape. The graphite flakes do not take place near the interface due to carbon diffusion so crack does not form near the interface and the load is carried by steel wire. It can be said that the carbon diffusion contributes the fracture toughness of the interface and the cast iron. Figure 8 shows that the fiber behaves a ductile role in the composite since a typical microvoid coalescence failure morphology was observed at the fracture surface of the fiber.

Increasing fracture toughness of gray cast iron by reinforcing steel wires was attributed to two mechanisms; fiber bridging and debonding of interface. When the load is applied, crack starts to extend into brittle gray cast iron and reaches to fibers. While the applied load increases, the fiber carries major part of the load. Then, the cross section of the fiber (app. 3.25 mm) decreased due to the plastic deformation of the fiber as shown in Fig. 9. The fibers tend to locally restrain crack extension. The local restrain could be the result of crack front blunting due to the debonding of

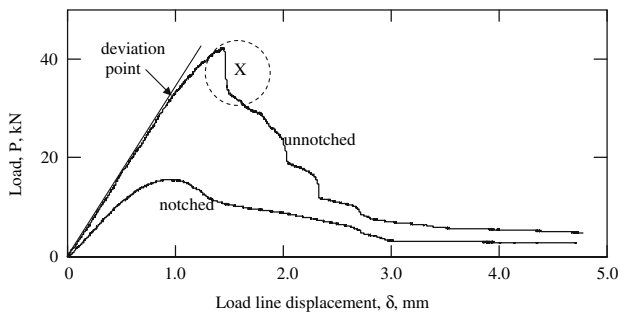

Fig. 7 Load–load line displacement curves notched and unnotched composites with $V_f = 0.08$

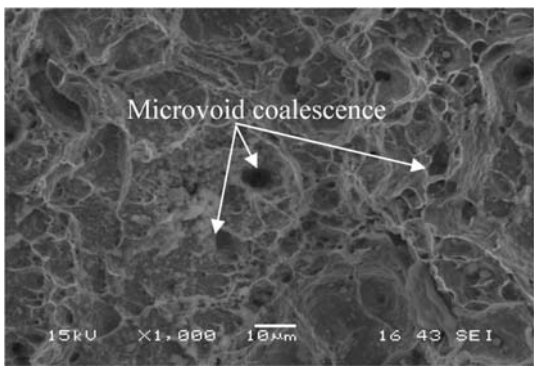

Fig. 8 Microvoid coalescence at the fracture surface of the fiber

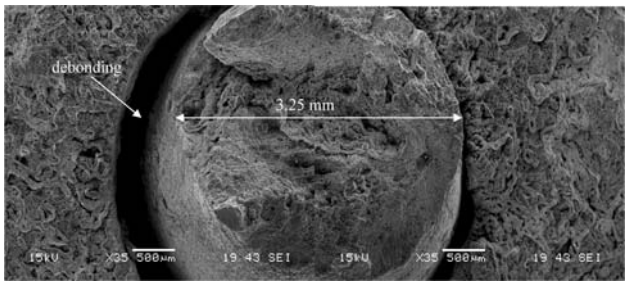

Fig. 9 Debonding of the interface between the matrix and the fiber, also the plastic deformation of the fiber

the interface and fiber breaks at the end [1, 4]. This can be concluded from the Fig. 7. As it is shown in Fig. 7, load increases linearly at the beginning of load-deflection curve then some deviation is observed up to the maximum load due to the plastic deformation of the steel fiber. The plastic deformation of fiber causes debonding of interface between steel fiber and cast iron. As shown in Fig. 7, after maximum loading, there is a sudden decrease in the load until the starting point of region X because of complete matrix cracking. In the region X, the decrement of the loading takes place suddenly due to fiber breakage of first bottom row [19, 20].

Microstructure

SEM (JSM-6400 Electron Microscope, JEOL) analysis was used to examine microstructure of the composite materials. Figure 10 shows the microstructure of the matrix, the interface and the fiber of the composite with $V_f = 0.05$. The transition region has approximately 600μm in length. The microstructure of the matrix phase (gray cast iron) is ferritic-pearlitic, that of the transition region has completely pearlite and that of the fiber is ferrite- pearlite. Transition region begin from gray cast iron side to fiber side. It is noted that there is a cabon diffusion from the gray cast iron to the fibers because pearlite phase takes place only in the transition region and there is present partially dissolved graphite flakes.

The Knopp hardness values were measured from the matrix side to the center of the fiber. Figure 11 shows the hardness profile. As it is seen that the hardness values increase during the transition region [21]. It is attributed that the carbon diffusion takes place from the matrix to the fiber, and forms the pearlite phase.

For future work, the carbon content of the steel fiber can be chosen to be sufficiently low that the graphite flakes were removed by carbon diffusion from the cast iron to the steel fibers during the solidification and cooling stages. By

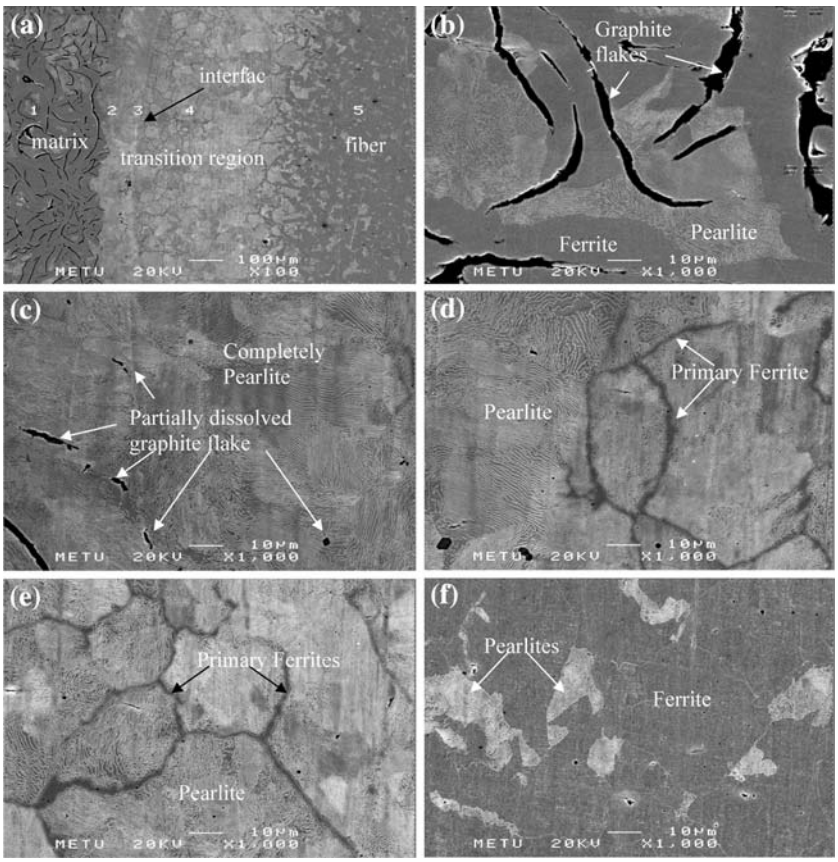

Fig. 10 (**a**) The matrix (point1), the transition region (between point 2 and 4), the interface(point3) and the fiber(5); Microstructure of (**b**) Matrix; (**c**), (**d**), (**e**), Transition region; (**f**) Fiber

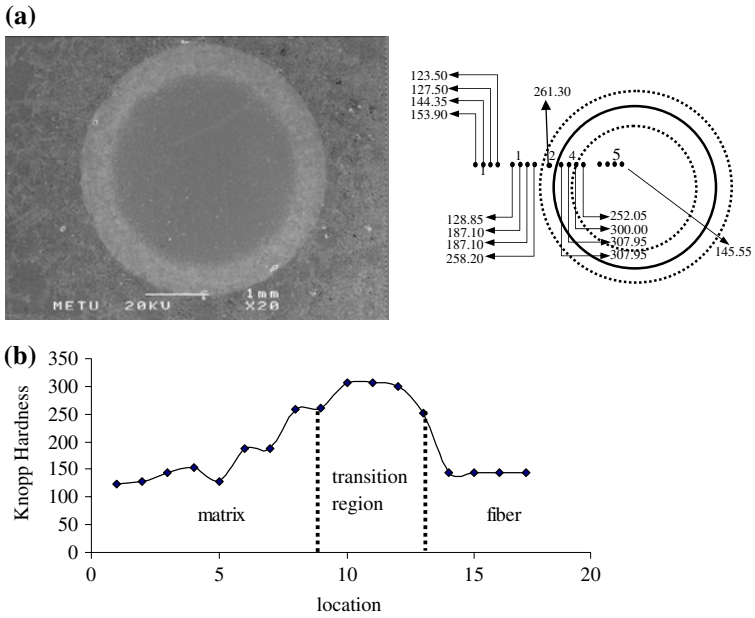

Fig. 11 (**a**) Hardness values (**b**)Variation of the Knoop hardness values from the matrix to the fiber

selecting the correct parameters such as casting condition, cooling rate, fiber orientation and heat treatment if necessary etc., having high strength and fracture toughness MMCs with completely graphite free matrix can be produced economically.

Conclusion

In this study, fracture toughness of the fiber reinforced composite where constituents are low tough and strength cast iron as a matrix and relatively high though and stregth steel wires as reinforcement, was investigated, and the following conclusions were obtained:

1. Flextural strength of the gray cast iron increases with adding the reinforcement and also increases with increasing the volume fraction of the reinforcement.
2. Plain strain fracture toughness of the composite, K_{IC} is greater than that of the cast iron and increases with increasing the volume fraction of reinforcement.
3. Compliance and *J*-integral methods are applied to determine the fracture toughness of the fiber reinforced composite for two distinct volume fractions of the reinforcements, $V_f = 0.05$ and 0.08. Values of the plain strain fracture toughness K_{IC}, are in good consistency for both methods.
4. Increasing fracture toughness of the composite is attributed to debonding of the interface and the plastic deformation of tough reinforcement.
5. Graphite free transition region having high hardness was observed due to the carbon diffusion.

References

1. Antolovich SD, Shete PM, Chanani GR (1972) ASTM STP514. American Society for Testing and Materials. p 114
2. Antolovich SD, Kasi K, Chanani GR (1972) ASTM STP514. American Society for Testing and Materials, p 135
3. Akdemir A, Arıkan H, Kuş R (2005) Mater Sci Technol 21:1099
4. Soboyejo WO, Ye F, Chen LC, Bahtishi N, Schwartz DS, Lederich RJ (1996) Acta Mater 44:2027
5. Chiang CR (2000) J Mater Sci 35:3161, doi: 10.1023/A:1004884322817
6. Qin S, Zhang G (2002) J Mater Sci 37:879, doi: 10.1023/A:1013868620945
7. Arpon R, Narciso J, Louis E, Cordovilla CG (2003) Mater Sci Technol 19:1225
8. Futato RJ, Aadland JD, van der Sluy WA, Lowe AL (1985) ASTM STP856. American Society for Testing and Materials, p 84
9. Prokopski G, Langier B (2000) Cement Concrete Res 30:1427
10. Panontin TL, Makino A, Williams JF (2000) Eng Fract Mech 67:293
11. Begley JA, Landes JD (1972) ASTM STP 514. American Society for Testing and Materials, p 1
12. Rice JR, Paris PC, Merkle JG (1973) ASTM STP 536. American Society for Testing and Materials, p 231
13. Hickerson J (1976) ASTM Committee Meeting E-24, Lake Buena Vista Fla
14. Gudas JP, Davis DA (1982) J Test Eval 10:252
15. Schwalbe KH, Hellman D, Heerens J, Knaack J, Roos JM (1985) ASTM STP856. American Society for Testing and Materials, p 338
16. Balton JD, Gant AJ (1998) J Mater Sci 33:939, doi: 10.1023/A:1004303609990
17. Neal BK, Priest RH (1985) ASTM STP 856. American Society for Testing and Materials, p 375
18. Gerberich WW (1971) J Mech Phys of Solids 19:71
19. Arikan H, Avci A, Akdemir A (2004) Polymer Test 23:615
20. Rohatgi A, Harach DJ, Vecchio KS, Harvey KP (2003) Acta Materialia 51:2933–2957
21. Şimşir M, Öztürk T, Doruk M (2004) Turkish J Eng Env Sci 28:397